2014 11th International Conference on Electrical Engineering, Computing Science and Automatic Control (CCE)

Triangulation-Based Indoor Robot Localization Using Extended FIR/Kalman Filtering

Moises Granados-Cruz, Juan Pomárico-Franquiz, Yuriy S. Shmaliy
Department of Electronics Engineering
Universidad de Guanajuato
Salamanca, 36885, Mexico
Email: shmaliy@ugto.mx

Luis J. Morales-Mendoza
Department of Electronics
Universidad Veracruzana
Poza Rica, 93390, Mexico
Email: javmorales@uv.mx

***Abstract*—A combined extended finite impulse response (EFIR) and Kalman (EFIR/Kalman) algorithm is proposed for mobile robot localization via triangulation. A distinctive advantage of the EFIR algorithm is that it completely ignores the noise statistics which are typically not well known to the engineer. Instead, it requires an optimal averaging interval of $N_{\rm opt}$ points. To run this algorithm, several initial Kalman estimates are used for the roughly set noise covariances. We consider a mobile robot travelling on an indoor floorspace and localized via triangulation with three nodes in a view. We show that the EFIR/Kalman filter is more accurate than the extended Kalman filter under the uncertain noise statistics and initial state.**

I. Introduction

Mobile robot applications require automatic localization or self-localization often in a way fast, accurate and low cost. Although the problem has been solved during decades by various methods [1], [2], the traditional *triangulation* is still used in many cases utilizing information obtained from three nodes having known coordinates. The first method implies that all stationary nodes are active (beacons) and the robot has a rotating receiver [1], [3]–[7]. The second method implies using passive landmarks or reflectors and rotating transmitter-receiver [1], [8], [9]. In the three-node triangulation system, three angles are often measured between the robot heading and the directions to the nodes [10]. These angles are coupled with the robot plane coordinates and heading by nonlinear equations. The equations can be solved for unknown robot coordinates and heading. Similarly, the algebraic equations can be solved for the unknown coordinates employing the trilateration methods and their modifications [11]. However, accuracy is commonly insufficient in noisy environments and optimal estimators are required.

The estimation theory offers several useful methods to the triangulation problem. One of the most common approaches is the extended Kalman filter (EKF) proposed by Cox [12] and others. The EKF was used in tracking and robotics extensively [1], [2], [13], [14] and has become a tool for moving vehicular navigation, tracking, localization, and self-localization [15], [16]. The benefit of the EKF resides in the following facts: 1) It solves the nonlinear equations while providing optimal denoising; 2) Its fast recursive algorithm requires small memory and is thus low-cost, and 3) It practically does not demonstrate divergence under the normal conditions of triangulation. However, EKF has also several widely recognized flaws: 1) Biased estimates, because noise is nonadditive in the triangulation formulation; 2) Divergence under the conditions of large nonlinearities and large noise [17] that is typical for boundaries of the floorspace area; 3) High sensitivity to noise; that is, the performance of EKF may be poor if the noise covariance matrices and initial errors are not well known [18]; and 4) Large errors under the industrial uncertainties and when noise is nonwhite Gaussian (heavy-tailed or Gaussian with outliers) [18].

Referring to these drawbacks, several alternative approaches have been developed in recent decades. The unscented Kalman filter (UKF) [19] demonstrates better performance when the state-space models is highly nonlinear. The hidden Markov model (HMM) filters [20] have appeared to be more useful for tracking [21]. A sequential Monte Carlo (SMC) method also known as a particle filter (PF) [22] was developed to estimate Bayesian models associated with Markov chains in discrete-time domain be especially useful for robot self-localization [23]. Another alternative to the EKF that has an infinite impulse response (IIR) is the extended finite impulse response (EFIR) filter recently proposed in [24]. Unlike the EKF, UKF, and optimal FIR (OFIR) filters [25], [26], the EFIR filter totally ignores the noise statistics and initial error statistics. Similarly to PFs, the EFIR filter exploits most recent past measurements which number is required to be optimal $N_{\rm opt}$ [27]. However, this technique is still not developed for robot localization and requires investigations. Below, we provide some results for localization via triangulation employing the FIR/Kalman filtering approach developed in [10].

II. Triangulation and filtering problem

Let us suppose that three nodes A, B, and C (beacons or passive marks) are mounted in an indoor space as shown in Fig. 1. A robot travels in the direction d with all three nodes in a view. A detailed schematic two-dimensional geometry of a moving robot is given in Figure 2. A node $\mathrm{B}(0,0)$ is placed in the corner that is a center of the indoor space planar Cartesian coordinates and two other nodes have coordinates $\mathrm{A}(0,y_1)$ and $\mathrm{C}(x_3,0)$. A robot travels in its own planar Cartesian coordinates $(x_{\rm r},y_{\rm r})$ with a center at $M(x,y)$; that is, the robot direction always coincides with axis $x_{\rm r}$. All nodes are observable by a robot or otherwise the nodes can observe a robot. The angles φ_1, φ_2, and φ_3 between axis $x_{\rm r}$ and the directions to the relevant nodes are supposed to be measurable by commercially available means. The robot

978–1–4799–6230–3/14/$31.00 ©

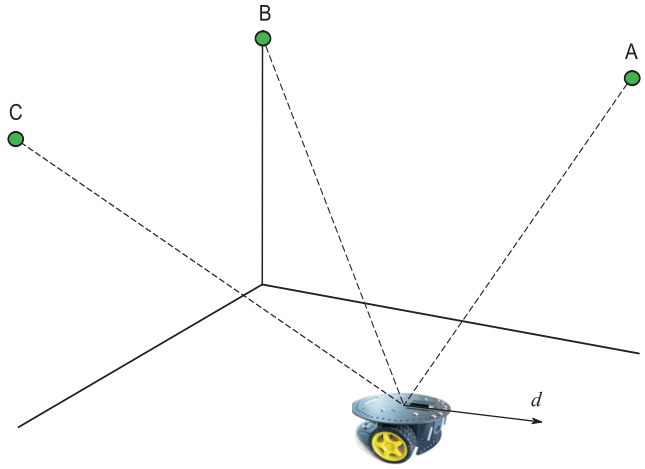

Fig. 1. A mobile robot platform traveling on an indoor floorspace in the direction d with the three nodes A, B, and C in a view.

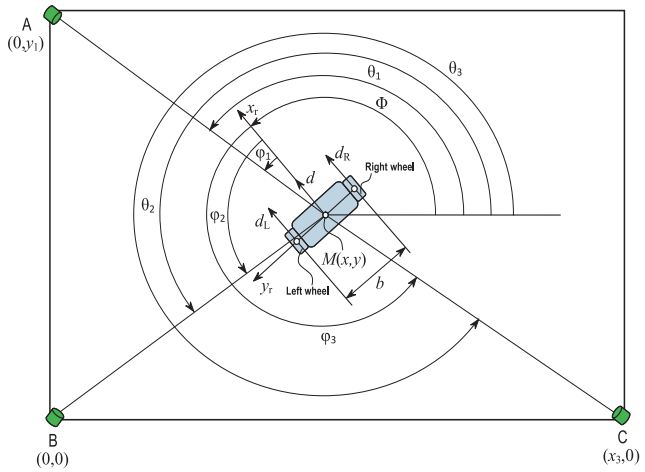

Fig. 2. Schematic two-dimensional geometry of a robot traveling on an indoor floorspace (Fig. 1).

behavior is controlled by left and right wheels installed at a distance b and the stabilizing wheel is not shown. The incremental distances robot travels by these wheels are d_{L} and d_{R}, respectively.

The incremental distance d_n at the mid-axis point and the incremental change ϕ_n in pose can be found at discrete time index n from the robot odometry as

$$d_n = \frac{1}{2}(d_{\mathrm{R}n} + d_{\mathrm{L}n})\,, \tag{1}$$

$$\phi_n = \arctan\frac{d_{\mathrm{R}n} - d_{\mathrm{L}n}}{b} \cong \frac{1}{b}(d_{\mathrm{R}n} - d_{\mathrm{L}n})\,. \tag{2}$$

In turn, the unknown coordinates x_n and y_n and pose Φ_n can be obtained by the robot kinematics with equations

$$f_{1n} = x_n = x_{n-1} + d_n \cos\left(\Phi_{n-1} + \frac{1}{2}\phi_n\right)\,, \tag{3}$$

$$f_{2n} = y_n = y_{n-1} + d_n \sin\left(\Phi_{n-1} + \frac{1}{2}\phi_n\right)\,, \tag{4}$$

$$f_{3n} = \Phi_n = \Phi_{n-1} + \phi_n\,, \tag{5}$$

in which the values x_{n-1}, y_{n-1}, and Φ_{n-1} at time $n-1$ are projected to time n by the time-variant incremental distances $d_{\mathrm{L}n}$ and $d_{\mathrm{R}n}$ via (1) and (2). Note that all the values in (3)-(5) are practically not exact and have some additive random components.

In the triangulation problem illustrated in Fig. 2, state variables x_n, y_n, and Φ_n are observable indirectly via the measured angles φ_{1n}, φ_{2n}, and φ_{3n} as

$$\varphi_{in} = \theta_{in} - \Phi_n\,, \tag{6}$$

where $i = 1, 2, 3$ and the exactly known $\bmod 2\pi$ angles θ_{1n}, θ_{2n}, and θ_{3n} existing from $-\pi$ to π are given by

$$\theta_{in} = \begin{cases} \arctan\frac{Q_{in}}{I_{in}}\,, & I_{in} \geqslant 0 \\ \arctan\frac{Q_{in}}{I_{in}} \pm \pi\,, & I_{in} < 0\,, \begin{cases} Q_{in} \geqslant 0 \\ Q_{in} < 0 \end{cases} \end{cases}, \tag{7}$$

where $Q_{in} = y_i - y_n$, $I_{in} = x_i - x_n$, and the node known coordinates y_i and x_i are: $y_1 \neq 0$, $y_2 = y_3 = 0$, $x_1 = x_2 = 0$, and $x_3 \neq 0$.

A solution to (6) gives us the robot location, $\tilde{x}_n$ and $\tilde{y}_n$, and pose $\tilde{\Phi}_n$ corrupted by noise:

$$\mathrm{tg}\,\tilde{\Phi}_n = \frac{A_n \cos\varphi_{1n} - \sin\varphi_{3n}}{A_n \sin\varphi_{1n} + \cos\varphi_{3n}}\,, \tag{8}$$

$$\tilde{x}_n = \frac{x_3\,\mathrm{tg}\,(\varphi_{3n} + \tilde{\Phi}_n)}{\mathrm{tg}\,(\varphi_{3n} + \tilde{\Phi}_n) - \mathrm{tg}\,(\varphi_{2n} + \tilde{\Phi}_n)}\,, \tag{9}$$

$$\tilde{y}_n = \tilde{x}_n\,\mathrm{tg}\,(\varphi_{2n} + \tilde{\Phi}_n)\,, \tag{10}$$

where

$$A_n = \frac{y_1}{x_3}\frac{\sin(\varphi_{3n} - \varphi_{2n})}{\sin(\varphi_{2n} - \varphi_{1n})} \tag{11}$$

and $\tilde{\Phi}_n$ is the $\bmod 2\pi$ angle specified similarly to (7). In this paper, we use $\tilde{x}_n$, $\tilde{y}_n$, and $\tilde{\Phi}_n$ as reference noisy "linear" measurements united in a vector $\mathbf{y}_n = [\,\tilde{x}_n\ \tilde{y}_n\ \tilde{\Phi}_n\,]^T$.

A. Triangulation State-Space Model

We now introduce a state vector $\mathbf{x}_n = [\,x_n\ y_n\ \Phi_n\,]^T$ of unknown variables and an input vector $\mathbf{u}_n = [\,d_{\mathrm{L}n}\ d_{\mathrm{R}n}\,]^T$ of incremental distances. We suppose that random components in these values are zero mean white Gaussian and uncorrelated. We unite these components in a state noise vector $\mathbf{w}_n = [\,w_{xn}\ w_{yn}\ w_{\Phi n}\,]^T$ and an input noise vector $\mathbf{e}_n = [\,e_{\mathrm{L}n}\ e_{\mathrm{R}n}\,]^T$. Following (3)-(5), the robot nonlinear state equation can thus be written as

$$\mathbf{x}_n = \mathbf{f}_n(\mathbf{x}_{n-1}, \mathbf{u}_n, \mathbf{w}_n, \mathbf{e}_n)\,, \tag{12}$$

where $\mathbf{f}_n = [\,f_{1n}\ f_{2n}\ f_{3n}\,]^T$ has components given by (3)-(5). Noise vectors $\mathbf{w}_n$ and $\mathbf{e}_n$ are zero mean, $E\{\mathbf{w}_n\} = \mathbf{0}$ and $E\{\mathbf{e}_n\} = \mathbf{0}$, have the covariances, $\mathbf{Q} = E\{\mathbf{w}_n\mathbf{w}_n^T\}$ and $\mathbf{L} = E\{\mathbf{e}_n\mathbf{e}_n^T\}$, and a property $E\{\mathbf{w}_i\mathbf{e}_j^T\} = \mathbf{0}$ for all i and j.

For the observation vector $\mathbf{z}_n = [\,\varphi_{1n}\ \varphi_{2n}\ \varphi_{3n}\,]^T$, nonlinear function vector $\mathbf{h}_n(\mathbf{x}_n) = [\,\theta_{1n} - \Phi_n\ \theta_{2n} - \Phi_n\ \theta_{3n} - \Phi_n\,]^T$, and measurement additive noise vector $\mathbf{v}_n = [\,v_{1n}\ v_{2n}\ v_{3n}\,]^T$, the state observation equation becomes

$$\mathbf{z}_n = \mathbf{h}_n(\mathbf{x}_n) + \mathbf{v}_n\,, \tag{13}$$

in which noise $\mathbf{v}_n$ is also supposed to be white Gaussian with zero mean $E\{\mathbf{v}_n\} = \mathbf{0}$, the covariance $\mathbf{R} = E\{\mathbf{v}_n\mathbf{v}_n^T\}$, and properties $E\{\mathbf{v}_i\mathbf{w}_j^T\} = \mathbf{0}$ and $E\{\mathbf{v}_i\mathbf{e}_j^T\} = \mathbf{0}$ for all i and j. The robot stochastic dynamics is thus represented with the state-space model (12) and (13).

B. Expanded state-space model

In order to apply Kalman filtering, the nonlinear state-space model (12) and (13) needs to be expanded to the first-order Taylor series. With respect to (12), such an expansion can be provided at $n-1$ as

$$\mathbf{f}_n = \mathbf{F}_n\mathbf{x}_{n-1} + \bar{\mathbf{u}}_n + \mathbf{W}_n\mathbf{w}_n + \mathbf{E}_n\mathbf{e}_n\,, \tag{14}$$

where $\hat{\mathbf{x}}_n$ is the estimate of $\mathbf{x}_n$. Here, $\mathbf{F}_n = \frac{\partial \mathbf{f}_n}{\partial \mathbf{x}}\big|_{\hat{\mathbf{x}}_{n-1}}$, $\mathbf{W}_n = \frac{\partial \mathbf{f}_n}{\partial \mathbf{w}}\big|_{\hat{\mathbf{x}}_{n-1}}$, and $\mathbf{E}_n = \frac{\partial \mathbf{f}_n}{\partial \mathbf{e}}\big|_{\hat{\mathbf{x}}_n^-}$ are Jacobian and $\bar{\mathbf{u}}_n = \mathbf{f}_n(\hat{\mathbf{x}}_{n-1}, \mathbf{u}_n, \mathbf{0}, \mathbf{0}) - \mathbf{F}_n\hat{\mathbf{x}}_{n-1}$ is known. An expansion (14) implies that an incremental difference $\mathbf{u}_n - \mathbf{u}_{n-1}$ is insignificant on a unit time step and can thus be neglected. Yet, because all of the values are supposed to be known exactly at $n-1$, we set $\mathbf{w}_{n-1} = \mathbf{0}$ and $\mathbf{e}_{n-1} = \mathbf{0}$. Matrix $\mathbf{F}_n = \frac{\partial \mathbf{f}_n}{\partial \mathbf{x}}\big|_{\hat{\mathbf{x}}_{n-1}}$ can be written as

$$\mathbf{F}_n = \begin{bmatrix} 1 & 0 & -d_n \sin(\hat{\Phi}_{n-1} + \frac{\phi_n}{2}) \\ 0 & 1 & d_n \cos(\hat{\Phi}_{n-1} + \frac{\phi_n}{2}) \\ 0 & 0 & 1 \end{bmatrix}, \tag{15}$$

where d_n is given by (1), ϕ_n by (2), and $\hat{\Phi}_{n-1}$ is the pose estimate at $n-1$.

Because noise $\mathbf{w}_n$ is additive with respect to the components of $\mathbf{x}_n$ in (3)-(5) and $\mathbf{w}_{n-1} = \mathbf{0}$, we also have

$$\mathbf{W}_n = \mathbf{F}_n \tag{16}$$

and transform the input matrix $\mathbf{E}_n = \frac{\partial \mathbf{f}_n}{\partial \mathbf{e}}\big|_{\mathbf{e}_{n-1}, \hat{\mathbf{x}}_n^-}$ to

$$\mathbf{E}_n = \begin{bmatrix} E_{11n} & E_{12n} \\ E_{21n} & E_{22n} \\ -\frac{1}{b} & \frac{1}{b} \end{bmatrix}, \tag{17}$$

where $E_{11n} = \frac{1}{2}\cos\left(\hat{\Phi}_n^- + \frac{\phi_n}{2}\right) + \frac{d_n}{2b}\sin\left(\hat{\Phi}_n^- + \frac{\phi_n}{2}\right)$, $E_{12n} = \frac{1}{2}\cos\left(\hat{\Phi}_n^- + \frac{\phi_n}{2}\right) - \frac{d_n}{2b}\sin\left(\hat{\Phi}_n^- + \frac{\phi_n}{2}\right)$, $E_{21n} = \frac{1}{2}\sin\left(\hat{\Phi}_n^- + \frac{\phi_n}{2}\right) - \frac{d_n}{2b}\cos\left(\hat{\Phi}_n^- + \frac{\phi_n}{2}\right)$, and $E_{22n} = \frac{1}{2}\sin\left(\hat{\Phi}_n^- + \frac{\phi_n}{2}\right) + \frac{d_n}{2b}\cos\left(\hat{\Phi}_n^- + \frac{\phi_n}{2}\right)$.

Reasoning similarly, we expand $\mathbf{h}_n(\mathbf{x}_n)$ at n as

$$\mathbf{h}_n(\mathbf{x}_n) = \mathbf{H}_n\mathbf{x}_n + \bar{\mathbf{z}}_n\,, \tag{18}$$

where $\mathbf{H}_n = \frac{\partial \mathbf{h}_n}{\partial \mathbf{x}}\big|_{\hat{\mathbf{x}}_n^-}$ is Jacobian,

$$\mathbf{H}_n = \begin{bmatrix} \frac{y_1 - \hat{y}_n^-}{(\hat{x}_n^-)^2 + (y_1 - \hat{y}_n^-)^2} & \frac{\hat{x}_n^-}{(\hat{x}_n^-)^2 + (y_1 - \hat{y}_n^-)^2} & -1 \\ \frac{-\hat{y}_n^-}{(\hat{x}_n^-)^2 + (\hat{y}_n^-)^2} & \frac{\hat{x}_n^-}{(\hat{x}_n^-)^2 + (\hat{y}_n^-)^2} & -1 \\ \frac{-\hat{y}_n^-}{(x_3 - \hat{x}_n^-)^2 + (\hat{y}_n^-)^2} & \frac{-x_3 + \hat{x}_n^-}{(x_3 - \hat{x}_n^-)^2 + (\hat{y}_n^-)^2} & -1 \end{bmatrix}, \tag{19}$$

and $\bar{\mathbf{z}}_n = \mathbf{h}_n(\hat{\mathbf{x}}_n^-) - \mathbf{H}_n\hat{\mathbf{x}}_n^-$ is known.

TABLE I. EFIR FILTERING ALGORITHM

Input: $\mathbf{z}_n$, $\mathbf{y}_n$, K, N
for $n = N-1 : M$ **do**
  $m = n - N + 1, \quad s = m + K - 1$
  $\tilde{\mathbf{x}}_s = \begin{cases} \mathbf{y}_s\,, & \textbf{if} \quad s < N-1 \\ \hat{\mathbf{x}}_s\,, & \textbf{if} \quad s \geqslant N-1 \end{cases}$
  $\mathbf{G}_s = \mathbf{F}_s\mathbf{F}_{s-1}(\mathbf{H}_{s,m}^T\mathbf{H}_{s,m})^{-1}\mathbf{F}_{s-1}^T\mathbf{F}_s^T$
  for $l = m + K : n$ **do**
    $\tilde{\mathbf{x}}_l^- = \mathbf{f}_l(\tilde{\mathbf{x}}_{l-1}, \mathbf{u}_l, \mathbf{0}, \mathbf{0})$
    $\mathbf{G}_l = [\mathbf{H}_l^T\mathbf{H}_l + (\mathbf{F}_l\mathbf{G}_{l-1}\mathbf{F}_l^T)^{-1}]^{-1}$
    $\mathbf{K}_l = \mathbf{G}_l\mathbf{H}_l^T$
    $\tilde{\mathbf{x}}_l = \tilde{\mathbf{x}}_l^- + \mathbf{K}_l[\mathbf{z}_l - \mathbf{h}_l(\tilde{\mathbf{x}}_l^-)]$
  and for
  $\hat{\mathbf{x}}_n = \tilde{\mathbf{x}}_n$
and for
Output: $\hat{\mathbf{x}}_n$

The expanded state-space model associated with the problem illustrated in Fig. 1 and Fig. 2 is thus the following:

$$\mathbf{x}_n = \mathbf{F}_n\mathbf{x}_{n-1} + \bar{\mathbf{u}}_n + \tilde{\mathbf{e}}_n + \tilde{\mathbf{w}}_n\,, \tag{20}$$
$$\mathbf{z}_n = \mathbf{H}_n\mathbf{x}_n + \bar{\mathbf{z}}_n + \mathbf{v}_n\,, \tag{21}$$

and the zero mean noise vectors $\tilde{\mathbf{w}}_n = \mathbf{W}_n\mathbf{w}_n$ and $\tilde{\mathbf{e}}_n = \mathbf{E}_n\mathbf{e}_n$ have the covariances, respectively,

$$\tilde{\mathbf{Q}}_n = \mathbf{F}_n\mathbf{Q}\mathbf{F}_n^T\,, \tag{22}$$
$$\tilde{\mathbf{L}}_n = \mathbf{E}_n\mathbf{L}\mathbf{E}_n^T\,. \tag{23}$$

The prior estimation error $\mathbf{P}_n^-$ and estimation error $\mathbf{P}_n$ are specified by

$$\mathbf{P}_n^- = E\{(\mathbf{x}_n - \hat{\mathbf{x}}_n^-)(\mathbf{x}_n - \hat{\mathbf{x}}_n^-)^T\,, \tag{24}$$
$$\mathbf{P}_n = E\{(\mathbf{x}_n - \hat{\mathbf{x}}_n)(\mathbf{x}_n - \hat{\mathbf{x}}_n)^T\,, \tag{25}$$

where $\hat{\mathbf{x}}_n^-$ and $\hat{\mathbf{x}}_n$ can be either EFIR or EKF estimate.

III. EXTENDED UFIR FILTERING

For the expanded state-space model (20) and (21), the EKF can be applied straightforwardly. Unlike the recursive EKF, the iterative EFIR filter [24] utilizes measurements $\mathbf{z}_n$ available on an interval of N past neighboring points from $m = n - N + 1$ to n. The EFIR filtering algorithm listed in Table I has the following specifics. For each time index n, the output is taken when $l = n$. The bias correction gain $\mathbf{K}_l$ is defined iteratively via the generalized noise power gain $\mathbf{G}_l$ ignoring the noise and error covariances. To avoid singularities, $\mathbf{G}_s$ is computed in the batch form. Linear measurement $\mathbf{y}_n$ is provided by (8)–(11). As can be seen, this algorithm needs only the horizon length N and the number of the states K to start computing and updating all the matrices, provided $\mathbf{z}_n$ and $\mathbf{y}_n$. No noise statistics are involved. The required N_{opt} can easily be determined using test measurements by minimizing (25). It has been shown in [27] that N_{opt} can also be found via measurements with no reference signal. The latter has a special significance for applications.

IV. Applications

As an example of applications, we simulate a mobil robot travelling stepwise on an indoor floorspace. The noise standard deviation in coordinates x_n and y_n is allowed to be 1 sm and in heading Φ_n to be 0.5°. Accordingly, we set $\sigma_x^2 = \sigma_y^2 = 10^{-4}$ m^2 and $\sigma_\Phi^2 = 7.62 \times 10^{-5}$ rad^2 in the diagonal matrix $\mathbf{Q}$. We also allow the noise standard deviation of 1 sm in the incremental distances $d_{\mathrm{L}n}$ and $d_{\mathrm{R}n}$ and set $\sigma_{\mathrm{L}}^2 = \sigma_{\mathrm{R}}^2 = 10^{-4}$ m^2 in the diagonal matrix $\mathbf{L}$. Assuming that measurements of all angles are provided with the noise standard deviation of 0.5°, we finally set $\sigma_{\varphi 1}^2 = \sigma_{\varphi 1}^2 = \sigma_{\varphi 1}^2 = 1.218 \times 10^{-3}$ rad^2 in the diagonal matrix $\mathbf{R}$. To show a consistency of EKF and EFIR estimates under the ideal conditions, we sketch in Fig. 3 the estimates of mobil robot location on an indoor floorspace. Here, we also show the location coordinates $\tilde{x}_n$ and $\tilde{y}_n$ obtained by (8)–(10). Fig. 4 shows the estimation errors by two filters. In this simulation, we suppose that the noise statistics are not well known and introduce the correction coefficient $p = 5$ to the noise matrices as $p^2\mathbf{Q}$, $\mathbf{R}/p^2$, and $\mathbf{L}/p^2$. We also admit a 10% error in the initial robot state for the EKF. Typical results shown in Fig. 3 reveal larger "slow" noise in the EKF estimates when $p > 1$. In an opposite case of $p < 1$ (not shown), the EKF demonstrates larger "fast" noise.

V. Conclusions

We can now summarize some trade-off between the EFIR and EKF algorithms in applications to the triangulation problem specialized by Fig. 2. The iterative EFIR filter ignores the noise statistics and initial error statistics that is a distinctive advantage against the EKF which requires all these measures as well as the initial state. We have demonstrated that when the noise covariances and initial state are specialized incorrectly that is typical fo many applications, then the EKF is able to produce large and even unacceptable errors. On the other hand, the optimal averaging interval N_{opt} for the EFIR filter can easily be determined via test measurements implying known state model. It may also be found even without a reference signal based on measurements. Although the EFIR/Kalman algorithm has proved its advantage against the EKF under the not fully known noise statistics and initial state, some questions still remain. There must be found a solution to overcome the boundary divergence. Also, the EFIR algorithm needs to be tested by other methods of localization and real measurements. We plan to report a progress in these investigations in near future.

References

[1] J. Borenstein, H. R. Everett, L. Feng, S. W. Lee, and R. H. Byrne, *Where am I? Sensors and Methods for Mobile Robot Positioning*, University of Michigan, 1996.

[2] A. Nüchter, *3D Robotic Mapping: The Simultaneous Localization and Mapping Problem with Six Degrees of Freedom*, Springer-Verlag, Berlin, 2009.

[3] S. Shoval and D. Sinriech, "Analysis of landmarks configuration for absolute positioning of autonomous vehicles," *J. Manufact. Syst.*, vol. 20, pp. 44–54, Jan. 2001.

[4] L. Cheng, C.-D. Wu, and Y.-Z. Zhang, "Indoor robot localization based on wireless sensor networks," *IEEE Trans. on Consumer Electron*., vol. 57, pp. 1099–1104, Mar. 2011.

[5] I. Amundson, J. Sallai, X. Koutsoukos, and Á. Lédeczi, "RF angle of arrival-based node localization," *Int. J. Sensor Networks*, vol. 9, no. 3/4, pp. 209–224, 2011.

[6] K. Sugihara, "Some Location Problems for Robot Navigation Problems Using a Single Camera," *Computer Vision, Graphics, Image Process*., vol. 42, pp. 112–129, Jan. 1988.

[7] E. Aitenbitchler and M. Mühlhäuser, "An IR local positioning system for smart items and devices," in: *Proc. 23rd Int. Conf. Distrib. Comput. Syst. Workshops*, 2003, pp. 334a??-339.

[8] E. Martín-Gorostiza, F.J. Meca, J.L. Lázaro-Galilea, E. Martos-Naya, F.B. Naranjo, and Ó. Esteban, "Coverage-Mapping Method Based on a Hardware Model for Mobile-Robot Positioning in Intelligent Spaces," *IEEE Trans. on Instrum. Measur*., vol. 59, pp. 266–282, Feb. 2010.

[9] Z. Wang and D. Gu, "Cooperative target tracking control of multiple robots," *IEEE Trans. on Industrial Electron*., vol. 59, pp. 3232–3240, Aug. 2012.

[10] J. Pomrico-Franquiz, S. H. Khan, and Y. S. Shmaliy, "Combined extended FIR/Kalman filtering for indoor robot localization via triangulation," *Measurement*, vol. 50, pp. 236?-243, Apr. 2014.

[11] J. Pomarico-Franquiz, Y. S. Shmaliy, "Accurate self-localization in RFID tag information grids using FIR filtering,? *IEEE Trans. Industrial Informatics,* vol. 10, pp. 1317?-1326, May 2014.

[12] H. Cox, "On the estimation of state variables and parameters for noisy dynamic systems," *IEEE Trans. Automat. Contr*., vol. AC-9, pp. 5–12, 1964.

[13] H. Cho and S.W. Kim, "Mobile robot localization using biased Chirp-Spread-Spectrum Ranging," *IEEE Trans. Industr. Electron*., vol. 57, pp. 2826–2835, Aug. 2010.

[14] Y. Motai and A. Kosaka, "Hand-eye calibration applied to viewpoint selection for robotic vision," *IEEE Trans. Industr. Electron*., vol. 55, pp. 3731–3741, Oct. 2008.

[15] Y. Bar-Shalom, X.-R. Li, and T. Kirubarajan, *Estimation with Applications to Tracking and Navigation*, New York: J. Wiley & Sons, 2001.

[16] S. Y. Chen, "Kalman filter for robot vision: a survey," *IEEE Trans. Industr. Electron*., vol. 59, pp. 4409–4420, Nov. 2012.

[17] R. J. Fitzgerald, "Divergence of the Kalman filter," *IEEE Trans. Autom. Contr.*, vol. AC-16, pp. 736–747, Jun. 1971.

[18] B. Gibbs, *Advanced Kalman Filtering, Least-Squares and Modeling*, New York: Wiley, 2011.

[19] S. J. Julier and J. K. Uhlmann, "A new extension of the Kalman filter to nonlinear systems," in: *Proc. SPIE*, vol. 3068, pp. 182a??-193, 1997.

[20] F. Martinerie and P. Forster, "Data association and tracking using hidden Markov models and dynamic programming," in: *Proc. IEEE Int. Conf. Acoust. Speech Signal Process. (ICASSP-92)*, San Francisco, CA, 1992, pp. 449–452.

[21] L. R. Rabiner and B.H. Juang, "An introduction to hidden Markov models," *IEEE Acoust. Speech Signal Process. Mag*., vol. 3, pp. 4–16, Jan. 1986.

[22] M. S. Arulampalam, S. Maskell, N. Gordon, and T. Clapp, "A tutorial on particle filters for online nonlinear/non-Gaussian Bayesian tracking," *IEEE Trans. on Signal Process*., vol. 50, pp. 174–188, Feb. 2002.

[23] D. Schulz, W. Burgard, D. Fox, and A.B. Cremers, "Tracking multiple moving targets with a mobile robot using particle filters and statistical data association," in: *IEEE Int. Conf. on Robotics Autom. (ICRA)*, vol. 2, 2001, pp. 1665–1670.

[24] Y. S. Shmaliy, "Suboptimal FIR filtering of nonlinear models in additive white Gaussian noise," *IEEE Trans. Signal Process*., vol. 60, pp. 5519–5527, Oct. 2012.

[25] W. H. Kwon and S. Han, *Receding Horizon Control: Model Predictive Control for State Models*, London: Springer, 2005.

[26] Y. S. Shmaliy, "Linear optimal FIR estimation of discrete time-invariant state-space models," *IEEE Trans. Signal Process*., vol. 58, pp. 3086–3096, Jun. 2010.

[27] F. Ramirez-Echeverria, A. Sarr, and Y. S. Shmaliy, "Optimal memory for discrete-time FIR filters in state space," *IEEE Trans. Signal Process*, vol. 62, pp. 557–561, Feb. 2014.

[28] Y. S. Shmaliy, "An iterative Kalman-like algorithm ignoring noise and initial conditions," *IEEE Trans. Signal Process*., vol. 59, pp. 2465–2473, Jun. 2011.

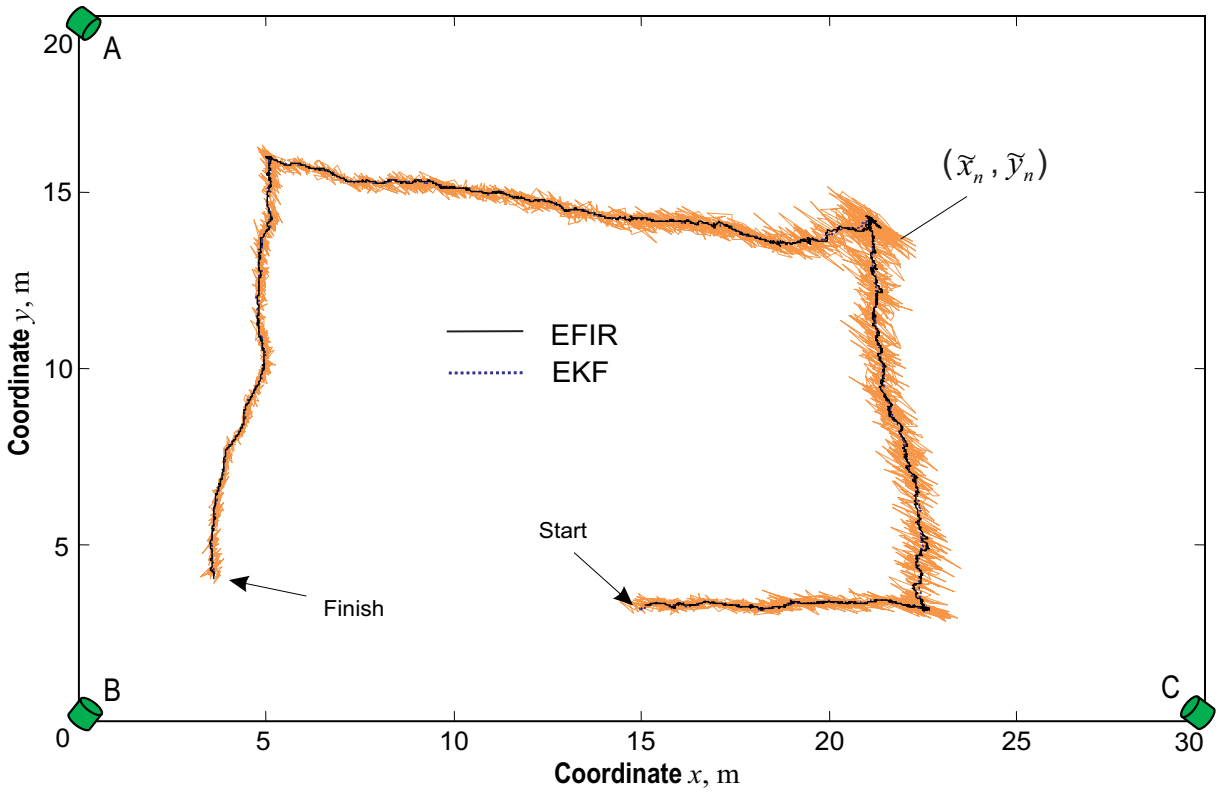

Fig. 3. Localization by (8)–(10) and extended filters of a robot traveling stepwise on a floorspace of dimensions (30×20) m in noisy environment. The EFIR and EKF produce consistent estimates.

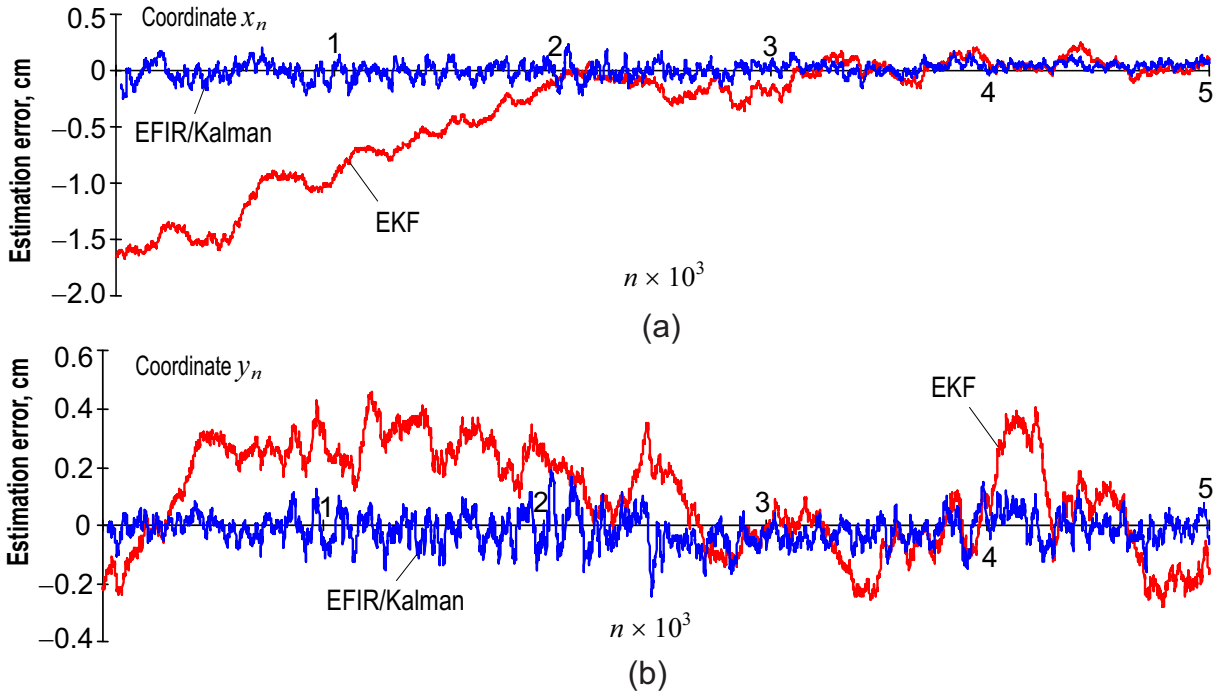

Fig. 4. Typical estimation errors as differences between the actual values and estimates shown in Fig. 3: (a) coordinate x_n and (b) coordinate y_n. The combined EFIR/Kalman filter produces lower errors than EKF ($p = 5$ and $1.1\mathbf{x}_0$) for x_n and y_n.